The GAW-CH Monitoring Programme at the Jungfraujoch

Final Report 01.01.2014 – 31.12.2017

Nicolas Bukowiecki, Erik Herrmann, Ghislain Motos, Günther Wehrle, Julia Schmale, Piotr Kupiszewski, Emanuel Hammer, Martin Gysel[1], Urs Baltensperger[1]

Paul Scherrer Institut, 5232 Villigen PSI

Martine Collaud Coen

MeteoSwiss, Chemin de l'aérologie, CH-1530 Payerne

[1]Programme leaders

Table of Contents

1   Project goals

Aerosols affect Earth's climate primarily by influencing the atmospheric energy budget through direct and indirect effects. Direct effects (aerosol – radiation interactions, ARI) refer to the scattering and absorption of radiation by aerosol particles. Indirect effects (aerosol – cloud interactions, ACI) refer to the role of particles

as cloud condensation nuclei (CCN) and ice-nucleating particles (INP). The number of CCN available under certain conditions affects droplet size in a cloud and thus cloud brightness and cloud life-time. The latter is also impacted by INPs which play a key role in initiating precipitation. The climate relevance of both direct and indirect effects results from their effect on the planetary albedo.

The Global Atmosphere Watch (GAW) programme is an activity overseen by the World Meteorological Organization (WMO). The goal of GAW is to ensure long-term measurements of key atmospheric constituents in order to detect trends and to develop an understanding of these trends. With respect to aerosols the objective of GAW is to determine the spatio-temporal distribution of aerosol properties related to climate forcing and air quality up to multi-decadal time scales. Since the atmospheric residence time of aerosol particles is relatively short, a large number of measuring stations are needed. The GAW monitoring network consists of 31 global (including the Jungfraujoch site) and about 400 regional stations. While global stations are expected to measure as many of the key variables as possible, the regional stations generally carry out a smaller set of observations. From May 2011 to April 2014, the aerosol programme at Jungfraujoch was also part of the European infrastructure project ACTRIS I3 FP7 (Aerosols, Clouds, and Trace gases Research Infra Structure), which is now followed by ACTRIS-2 IA H2020 (May 2015 to April 2019).

The Jungfraujoch aerosol observations are among the most complete worldwide (see Table 1). By the end of 2017 they reached over 22 years of continuous measurements for part of the observables (see Figure 1.1). On occasion of this anniversary, a review article was published, summarizing the two decades of aerosol monitoring and research at Jungfraujoch (Bukowiecki et al., 2016).

The following sections present the achievements within this time period, structured by the research plan presented in the project proposal.

Table 1: Current GAW aerosol monitoring instrumentation the high altitude research station Jungfraujoch

Instrument	Measured parameter
CPC (TSI 3772)	Particle number concentration (particle diameter $D_p > 10$ nm)
Nephelometer (TSI 3563)	Aerosol scattering and backscattering coefficient at three wavelengths
Nephelometer (Ecotech Aurora 3000)	
Nephelometer (Airphoton IN101), **acquired in Dec 2017**	
Aethalometer (AE-31. Magee Sci. Inc.)	Aerosol absorption coefficient at 7 wavelengths; mass concentration of equivalent black carbon equivalent (m_{eBC})
Aethalometer (AE33, Magee Sci. Inc.)	
MAAP	Aerosol absorption coefficient at 637 nm; mass concentration of equivalent black carbon equivalent (m_{eBC})
Filter packs	Aerosol major ionic composition (PM1 and TSP)
Fidas and HiVol[1]	Aerosol mass concentration, PM10 and TSP
Scanning Mobility Particle Sizer SMPS	Particle number size distribution ($D_p = 16 - 593$ nm)
Cloud Condensation Nuclei Counter, CCNC	CCN number concentrations at different supersaturations
Optical Particle Sizer (Grimm 1.108) **until Dec 2016**	Coarse mode number size distribution ($D_p = 0.3 - 10$ µm)
Optical Particle Sizer (TSI OPS 3300) **since Jan 2016**	

1) measured by EMPA
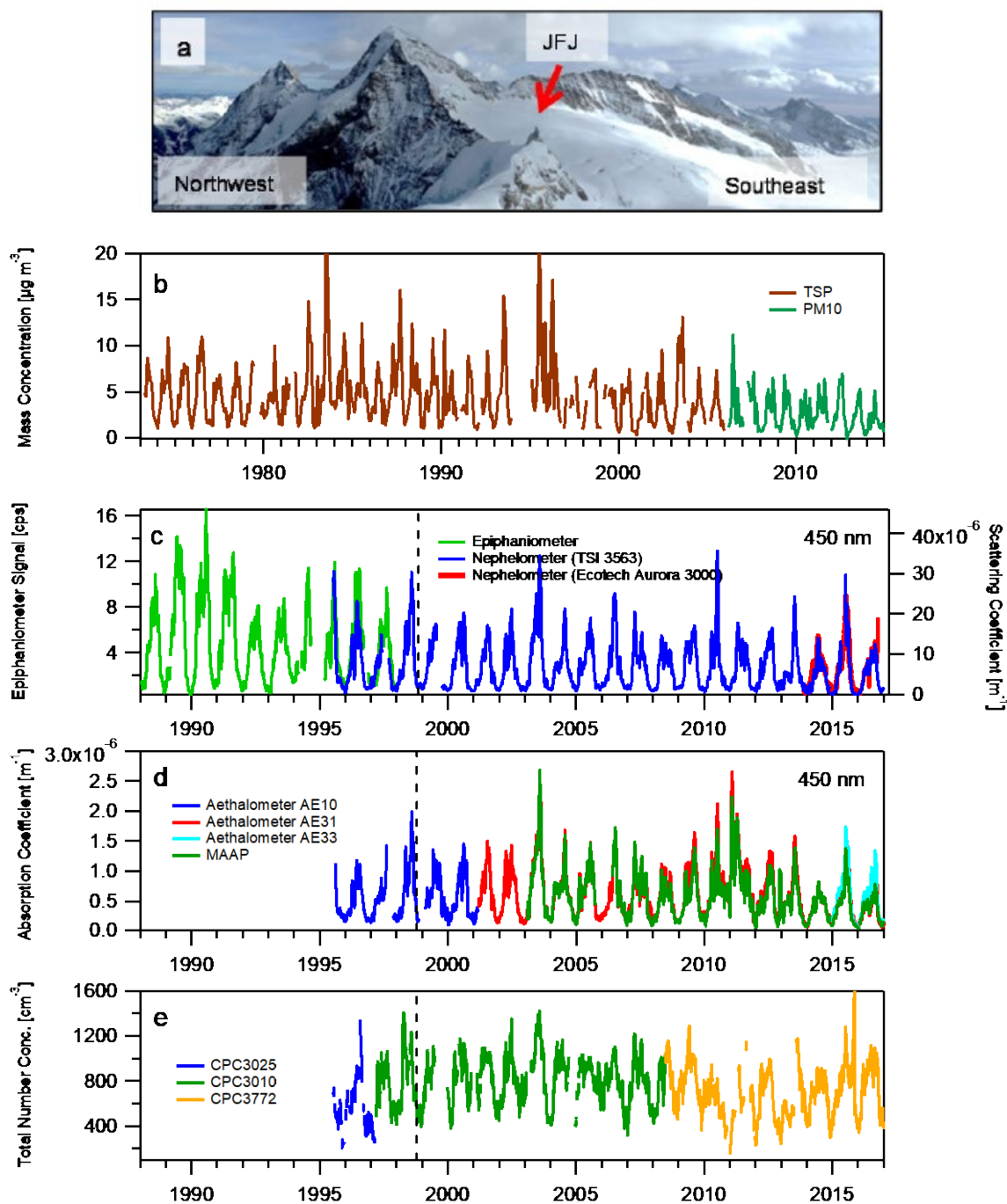
Fig. 1.1. Panel a: View of the station at Jungfraujoch (JFJ). Panels b–e: Temporal evolution of the continuously measured aerosol parameters at the Jungfraujoch. For TSP and PM10 monthly average values are shown, for the rest of the parameter the 30-day running average of the daily average values. The dashed vertical lines (Panels c–e) indicate that in January 1998, the entire aerosol laboratory was moved from the old JFJ research station (3454 m asl) to the JFJ Sphinx research station (3580 m asl) and a new inlet was employed. Gravimetric TSP and PM10 is sampled separately. Adapted from Bukowiecki et al., 2016.

2 Continuation and improvement of the monitoring activities

2.1 Operation, data archiving and quality assurance

During the project phase 2014 to 2017 the monitoring activities were performed as planned and delivered quality assured data with high temporal coverage. Touristic activities clearly influenced the data, especially during the summer season (see also Section 2.3).

The data are carefully analyzed, quality controlled and flagged and are transmitted on a periodic basis to the WDCA and ACTRIS data centres (EBAS), as illustrated in Figure 2.1.1.

JFJ Aerosol Data Chain (March 2018)
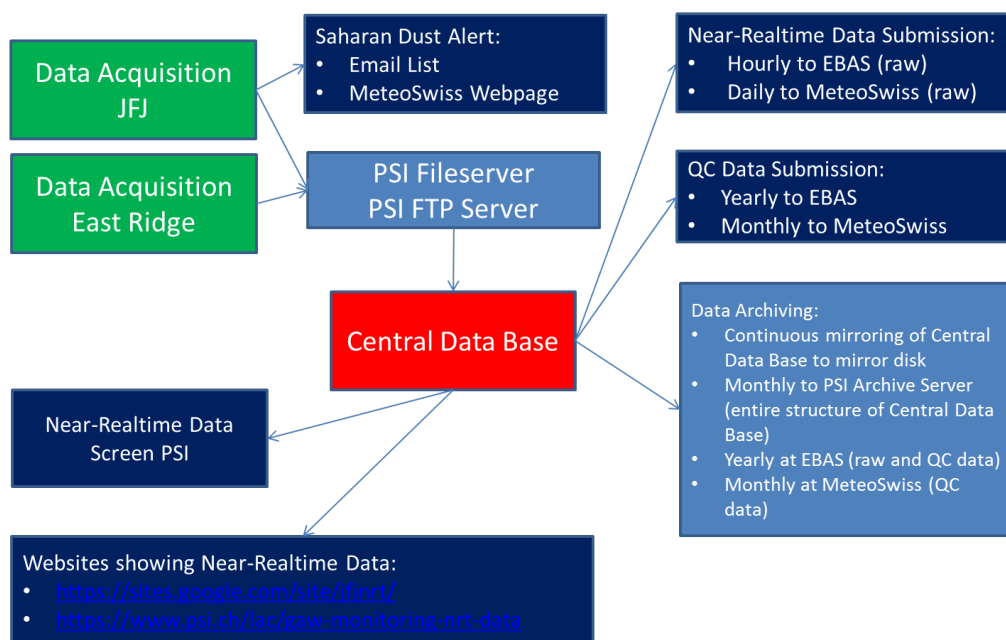
Fig. 2.1.1: Data Flow of JFJ Aerosol Measurements

Technical and monitoring network related activities 2014:

- We purchased a new AE-33 (Dual Spot 7-wavelength Aethalometer) to replace the old AE-31 which is reaching its end of lifetime. Parallel measurements have started mid-October 2014 and are ongoing.
- Our SMPS instrument (number size distribution measurements): participated at the mandatory ACTRIS (Phase 1) intercomparison workshop in Leipzig in May 2014 and successfully passed the intercomparison. In autumn 2014 the CPC of the SMPS was sent for repair due to technical problems. A new CPC 3775 was purchased for replacement, while the repaired CPC 3775 is running as standalone unit at the Jungfrau East Ridge. Data continuity and comparability was achieved via the comparison of the SMPS with the standalone CPC 3772 at the Sphinx.
- The previous PSI data base structure (operational since 1999) hosting the JFJ aerosol data reached its end of lifetime. PSI and MeteoSwiss initiated exploration of possibilities to integrate the JFJ GAW

aerosol measurements into the MeteoSwiss Data Warehouse, to make the data chain and the quality checks (joint process of MeteoSwiss and PSI) more efficient and powerful.

- The comprehensive data sets from the monitoring activities and the insights on process level from the research projects were used to validate and improve model simulations, inter alia as part of the EU project BACCHUS.

- Parallel measurements at the Jungfrau East Ridge (JER) started in October 2014, see Section 2.2.

Technical and monitoring network related activities 2015:

- In summer 2015 the JFJ aerosol data chain was redesigned, based on the specialized CPD software developed at NOAA (https://www.esrl.noaa.gov/gmd/aero/sw.html). Special focus was put on making the data chain and the quality checks (joint process of MeteoSwiss and PSI) more efficient and powerful. For an efficient data transfer between PSI and MeteoCH, the aerosol near real-time data are made available to MeteoCH via FTP (daily data files). The new data flow structure was carefully quality-checked by N. Bukowiecki and M. Collaud Coen.

- Our CPC 3772 instrument (particle number concentration) participated at the mandatory ACTRIS intercomparison workshop in Leipzig in November 2015. The unit passed the intercomparison, despite an undercounting of 7%. The unit was recalibrated and thereafter counted within <2% uncertainty compared to the Leipzig reference unit. This exemplifies the large benefit of these regular intercomparison efforts.

- In 2015 the study by Fröhlich et al. about 14 months of on-line chemical aerosol analysis at the JFJ was published. The results (see Section 2.4.4 of this report) illustrated the benefit of this type of measurements and its potential as a possible further addition to the monitoring programme.

Technical and monitoring network related activities 2016:

- After the redesign of the JFJ aerosol data chain in 2015, further features were introduced in 2016. Near-realtime (NRT) data submission to EBAS and ACTRIS data centers went live in July 2016 for the TSI nephelometer and the MAAP. The NRT data can be visually checked at the ACTRIS website.[1].

- 2016 was the first full year following the new workflow between PSI and MeteoSwiss, as defined in 2015. The unflagged aerosol near real-time data are made available to MeteoCH via FTP (daily data files), while the targeted interval for the submission of quality controlled data from PSI to MeteoSwiss is monthly (operational as of 2017).

- In 2016, several instruments participated in instrument intercomparison workshops at the European Center for Aerosol Calibration (ECAC) in Leipzig, which are mandatory for all stations within the ACTRIS network. In the current ACTRIS2 phase (2015-2019), it is required that every instrument participates in an ECAC intercomparison at least once. The AE33 aethalometer successfully passed the intercomparison in July 2016. Both JFJ nephelometers (TSI and Ecotech Aurora 3000) participated in the ECAC workshop in June 2016. The intercomparison revealed partial differences to the reference instrument for both instruments and the units were rescheduled for participation in 2017 (see separate section of this report). The actual temporal absence of the instruments from JFJ due to the workshop participation ranges between 2 weeks (only feasible if a PSI employee is

---

[1] http://actris.nilu.no/Content/?pageid=844fe06802f04a83a2d6b0e8b2a59fe2

available to travel with the instrument to Leipzig and back by car) and 2 months (in case of unfortunately frequent customs problems during unattended shipping). Unfortunately the participation of the CCNC in November 2016 was without success due to transport damage on the way to Leipzig.

- Overlapping measurements the old TSI Nephelometer (running since 1995) and the Ecotech Aurora 3000 Nephelometer purchased in 2013 showed that the Ecotech nephelometer is not capable to replace the TSI instrument with sufficient data quality at the low aerosol concentration levels. Detailed analysis of the data is shown in Section 2.3.

- Back in 2005, PSI added an Optical Particle Counter (Grimm OPC 1.108) to the monitoring instruments as in-kind contribution. Unfortunately this unit broke in 2015 and was no longer repairable because the model is not supported by the manufacturer anymore. Thus, a new Optical Particle Sizer (TSI OPS 3300) was purchased and installed in early 2016, as these data are of great use for many research questions.

Technical and monitoring network related activities 2017:

- In June 2017 the automated Saharan Dust Event (SDE) alert was reissued on the MeteoSwiss webpage (http://www.meteoswiss.admin.ch/home/climate/the-climate-of-switzerland/specialties-of-the-swiss-climate/saharan-dust-events.html). Since November 2017, the SDE alert is calculated with the AE33 aethalometer data and no longer with the AE31.

- Also in 2017, several instruments participated in instrument intercomparison workshops at the European Center for Aerosol Calibration (ECAC) in Leipzig, following the ACTRIS/ECAC QA rules. In January 2017, The AE31 aethalometer as well as the MAAP in November 2017 and the SMPS in May2017. Also in 2017, the actual temporal absence of the instruments from JFJ due to the workshop participation ranges between 2 weeks and 2 months.

- From September to December 2017, PSI tested an Airphoton nephelometer (model IN101) at JFJ and subsequently in the laboratory at PSI. The tests showed that the instrument is very suitable to measure under JFJ conditions, see Section 2.3. The unit was purchased in December 2017 in order to replace the existing two nephelometers.

2.2   Additional measurements at the Jungfrau East Ridge

In October 2014, an aethalometer (AE-33) and a condensation particle counter (TSI 3775) were installed at the Jungfrau East Ridge station (3705 m a.s.l., former Swisscom station), to measure aerosol microphysical properties. These measurements will be compared to those performed at the Sphinx Laboratory with a similar setup, to determine the impact of local pollution at Jungfraujoch and to investigate the small-scale spatial variability of aerosol parameters. Beside scientific interest, a major goal of these measurements is to assess the degree of local pollution at the Sphinx, i.e. the quantitative influence of these spikes on daily average of CPC and other data.

At the JFJ, the aerosol number concentration ($N_{>10\,nm}$) is sensitive to:

- PBL influenced air masses ("moderate" concentrations)
- New particle formation (bursts/"bananas" up to 20'000 cm^{-3})
- Helicopter exhaust (spikes up to 10'000 cm^{-3})

- Cigarette smoke from the tourist platform (spikes up to 10'000 cm^{-3})

The equivalent black carbon mass concentration is sensitive to:

- PBL influenced air masses ("moderate" concentrations)
- Local combustion processes in general (e.g. diesel generators)
- Snow cat emissions (only from snow cat used at Mönchsjochshütte, the snow cats used by the Jungfrau Railway are electrical)

Figure 2.2.1 shows a comparison of the total number concentration at both sites for a couple of days in autumn 2014. While concentrations are nearly identical during night-time, data from the Sphinx show large spikes during the day which indicate tourism-related local pollution (Fröhlich et al., 2015). By the use of an appropriate spike filter (Figure 2.2.2), pollution spikes can be filtered for those instruments with high time resolution (< 5 min). With this spike filter, high pollution days can be defined, e.g. as days with more than 8 strong peaks at JFJ and less than 2 strong peaks at JER. In the 3 years of parallel measurements (Oct 2014 to Oct 2017), the percentage of high local pollution days was 9%, and the averaged particle number concentration increased 25% during high pollution days compared to the filtered baseline.

Figure 2.2.3 shows the monthly frequency of high pollution days from 2014 – 2017, along with the number of visitors at the JFJ. It is clearly seen that in 2015 and 2016 both numbers correlate, while the number of high pollution days decreased in 2017. This is most likely attributed to signs that were installed on the Sphinx tourist platform with the invitation to the tourist to refrain from smoking.

The additional measurements at Jungfrau East Ridge are extremely helpful to quantitatively assess the influence of local pollution at JFJ. In addition to the focus on local emissions, we are currently working on the connection of the aerosol measurements at both sites to nearby ceilometer measurements, to assess the effect of local vertical transport on baseline differences between JFJ and JER.
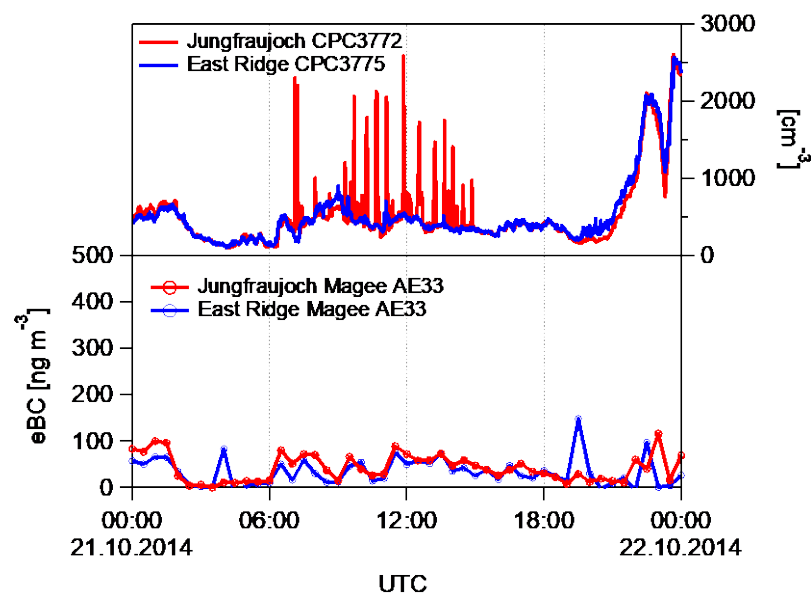
Fig. 2.2.1: Typical "high pollution day" at JFJ. Top panel: Aerosol number concentration (1-min time resolution). Bottom Panel: eBC mass concentration (30-min time resolution)
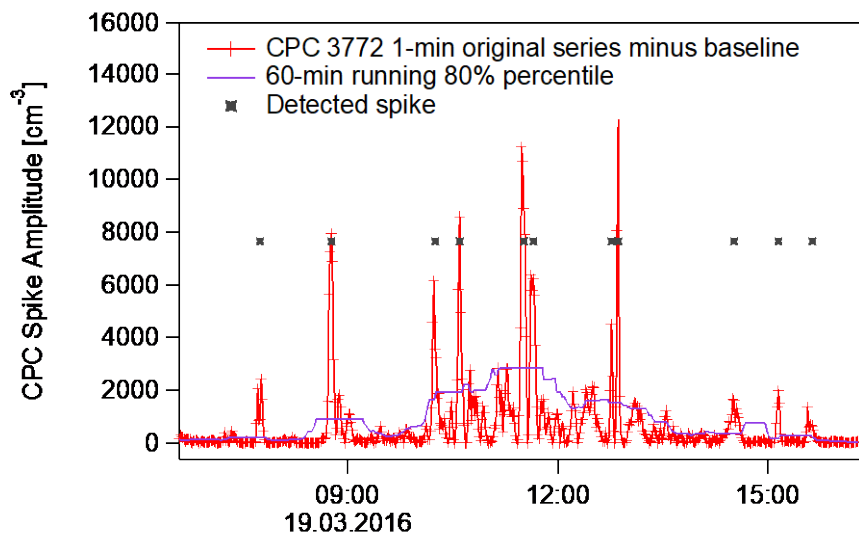
Fig. 2.2.2: Spike filter: 1) Calculate baseline (running 10-min 5th-percentile), 2) Subtract baseline to have the isolated «spike series», 3) Apply automated spike algorithm to define JFJ and JER spikes (running 60-min 80th-percentile smaller than original value of spike), 4) Analyze the spike frequency and quantitatively define the «JFJ high local pollution days» (more than 8 strong peaks at JFJ and less than 2 strong peaks at JER)
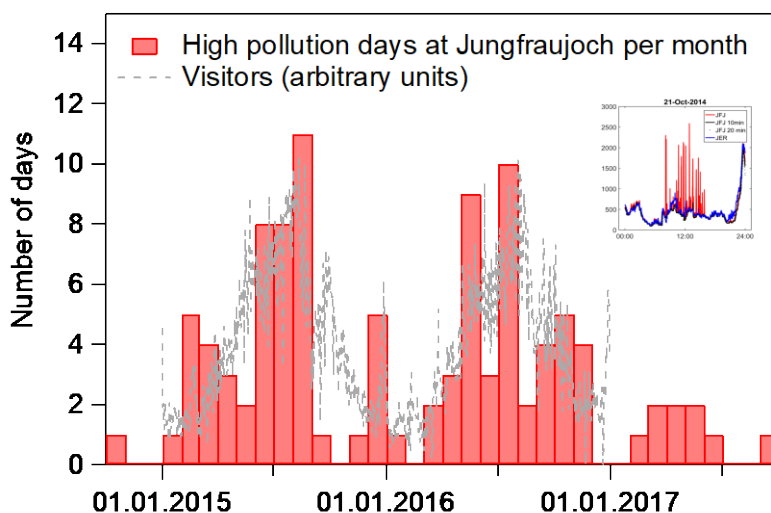
Fig. 2.2.3: High local pollution days at (more than 8 strong peaks at JFJ and less than 2 strong peaks at JER). At the time of this report the detailed visitor numbers for 2017 were not yet available. According press communications from the Jungfrau Railways the visitor frequency increased by 14% compared to 2016 (https://www.schweizeraktien.net/blog/2018/01/05/jungfraubahn-2017-wieder-ueber-1-mio-besucher-auf-dem-jungfraujoch-18203/).

Fig. 2.2.4:. Setup of the instruments at the former Swisscom station at Jungfraujoch East Ridge.

2.3   Nephelometer Intercomparison

At the Jungfraujoch research station, the TSI 3563 has been measuring since March 1999 and clearly presents an increase of the noise since 3-4 years and the most affected wavelength is the blue one at 450 nm. The instrument was completely revised during the intercomparison at Leipzig in June 2016 and some of the problems were considerably reduced.

The TSI company decided not to support the further development and the marketing of the nephelometer, while the Ecotech company developed two nephelometers since 2012. First intercomparisons (Müller et al., 2011) of both nephelometers seemed to be promising, resulting in only small differences between both instruments.

At the JFJ, an Aurora 3000 nephelometer from Ecotech has been measuring since July 2013 simultaneously with the TSI nephelometer. It performs a zero check once a week which lasts about 30 minutes (this was changed to daily in 2016, based on GAW/ACTRIS recommendations). Overall, it was found that the zero measurements of the Aurora 3000 showed quite large spread, especially for the total scatter (Figure 2.3.1), which has a large influence on the uncertainty of the measured scattering and backscatter coefficients.

The TSI and Ecotech scattering coefficients at 450 nm were compared for the July-December 2016 period, namely after the revision of the TSI instrument and the check of the Ecotech instrument during the Leipzig intercomparison. As can be seen in Figure 2.3.2, there is a very good correlation between the scattering coefficients of both instruments with increasing discrepancies for lower scattering coefficients ($< 5 \cdot 10^{-6}$ m^{-1}). The slopes of the fit between both instruments increase with wavelengths (0.98 @ 450 nm, 1.14 @ 550 nm and 0.60 @ 700 nm, the Ecotech scattering coefficient being reported to the TSI wavelengths with a theoretical exponent of -1), the Ecotech nephelometer measuring higher scattering coefficient than the TSI one for 550 and 700 nm.
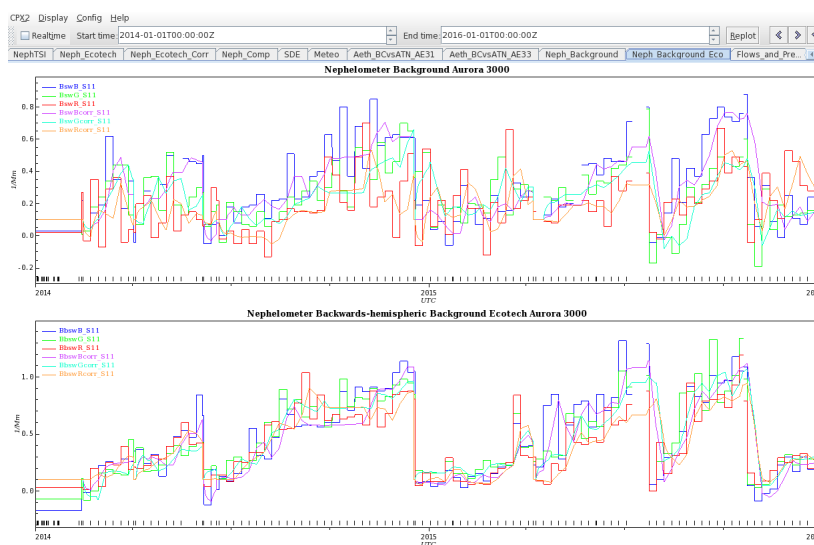
Fig. 2.3.1: Ecotech zero adjustment for the total and backwards scattering for 2014-1015.
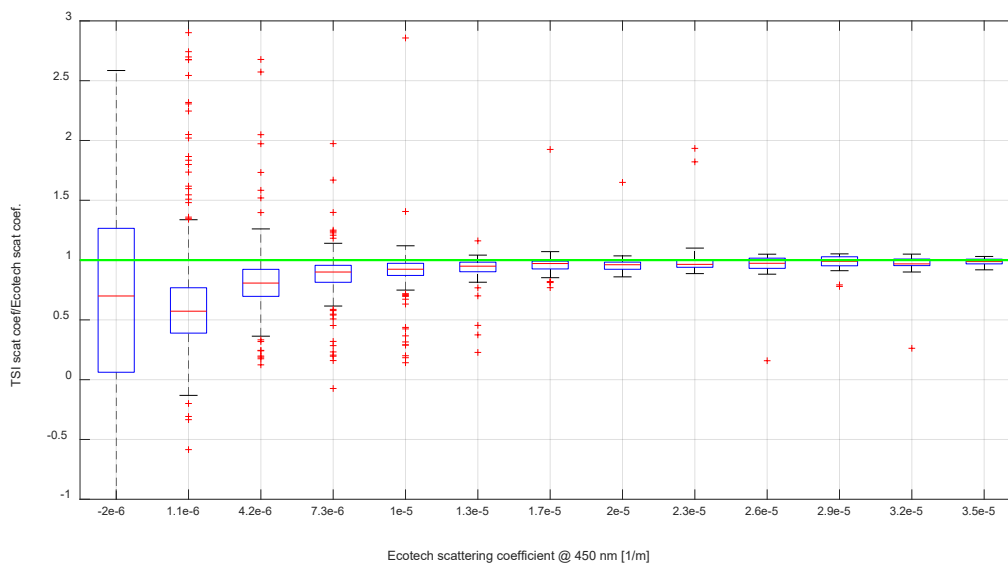
Fig.2.3.2: Statistics (median, quartiles, 5th and 95th percentiles as well as outliers) of the ratio between the scattering coefficients of the TSI and Ecotech nephelometers as a function of the Ecotech scattering coefficient.

While the coefficients themselves are well correlated, the discrepancy between the scattering Ångström exponents measured by the two instruments is much more pronounced. As can be seen in Figure 2.3.3, the Ecotech scattering Ångström exponent is systematically lower than the TSI one and has a different shape. This bad estimation of the wavelength dependence by the Ecotech nephelometer has some impact on the truncation correction that has to be applied to both instruments and impeded the detection of Saharan dust events (SDE). With the Ecotech scattering exponent being too low, SDE are not ideally detected which leads to an obviously unrealistic 10-fold increase of hours with SDE at the JFJ. A detailed inspection of the data proves that the method used to do the zero checking at the three wavelengths is the main cause of the

difficulties to measure the wavelength dependence at low aerosol concentrations. Several corrections of the algorithm to measure the zero values, of the scattering exponent calculation and of the SDE detection were applied to the dataset without success. The inability of the Ecotech nephelometer to measure the wavelength dependence at low aerosol concentration associated with the end of the TSI nephelometer production represents a real problem of all high and middle altitude stations around the world.
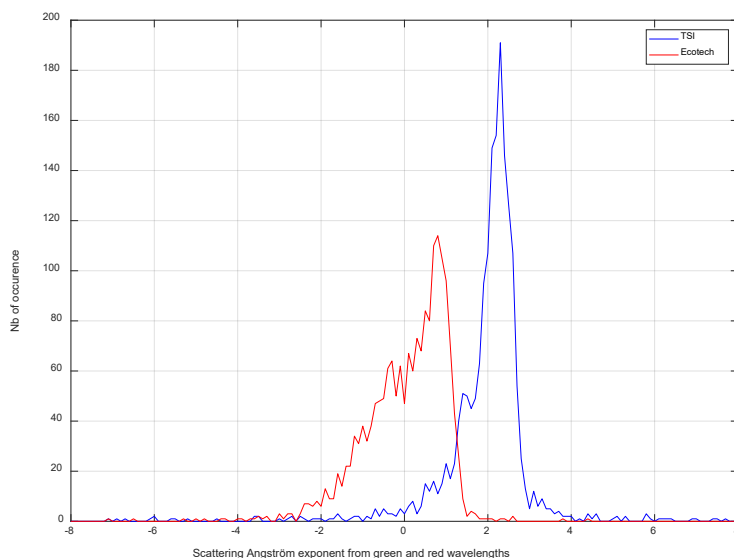
Fig. 2.3.3: Histograms of the scattering Ångström exponents for the TSI (blue) and Ecotech (red) nephelometers. The scattering exponents were obtained with the scattering coefficients at the green and red wavelengths. Similar results are found if a fit with the three wavelengths is applied.

From October to December, an Airphoton IN101 nephelometer was tested at JFJ. In contrast to the TSI and Ecotech nephelometer, the Airphoton IN101 has no movable parts (shutter etc.) and provides the reference and dark counts entirely by the novel arrangement of the optical and electronical components. This makes the unit more suitable for long-term monitoring. Figure 2.3.4 shows an example time series from all three nephelometers in their native time resolution and illustrates the excellent sensitivity of the IN101. After the tests at JFJ, the unit was also taken to PSI for further laboratory tests. The goal of these tests was to compare the experimental instrument response to the theoretical response from Mie theory. Figures 2.3.5 and 2.3.6 show a very good agreement of the instrument signal with theory. Given the excellent test results, the IN101 was purchased by the end of 2017 and is currently being implemented into the monitoring programme at the JFJ. The detailed data processing and correction algorithms are currently being defined as a collaboration between PSI, MeteoSwiss and the manufacturer.
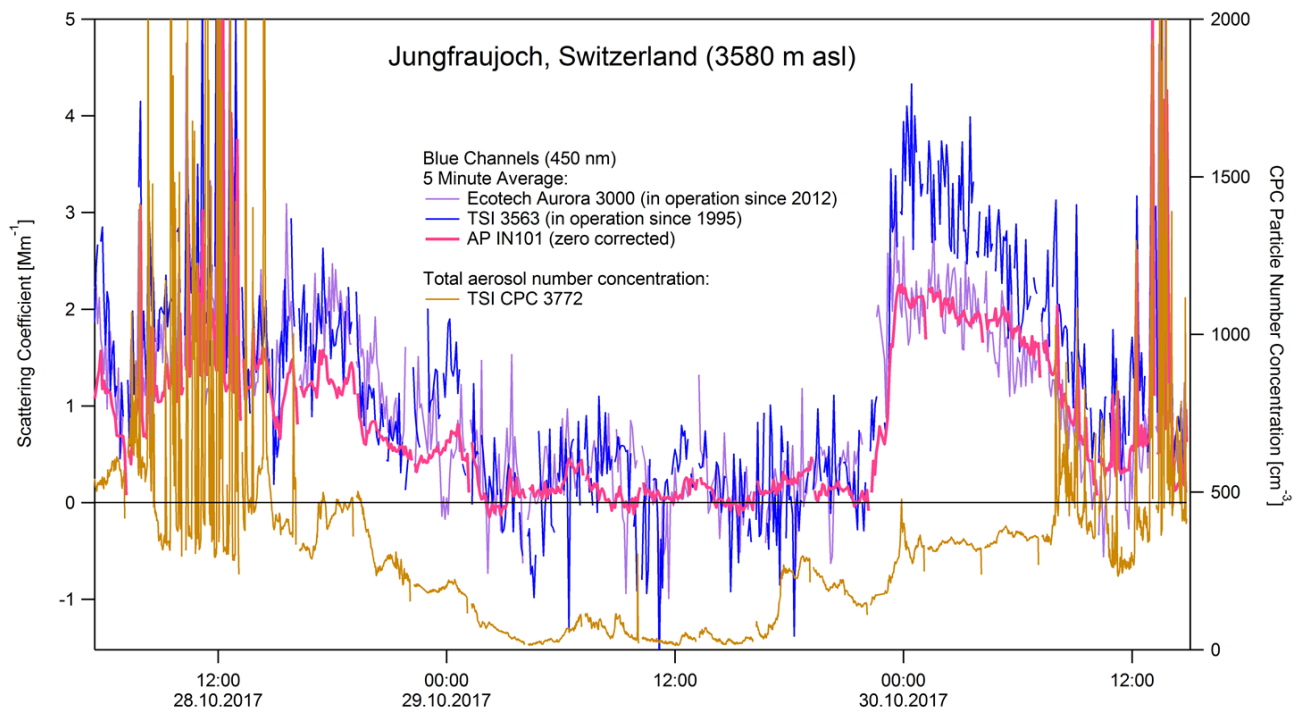
Fig 2.3.4: Comparison between the Airphoton IN101, the TSI 3563 and the Exotech Aurora 3000 nephelometers at the Jungfraujoch.
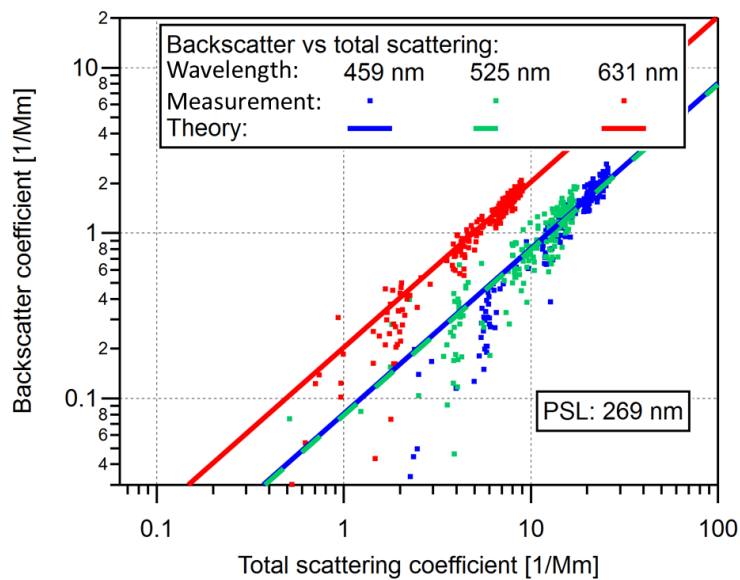
Fig. 2.3.5: Plot of the Airphoton IN101 nephelometer backscattering towards the total scattering coefficients for a laboratory experiment with PSL particles as well as the theoretical response.
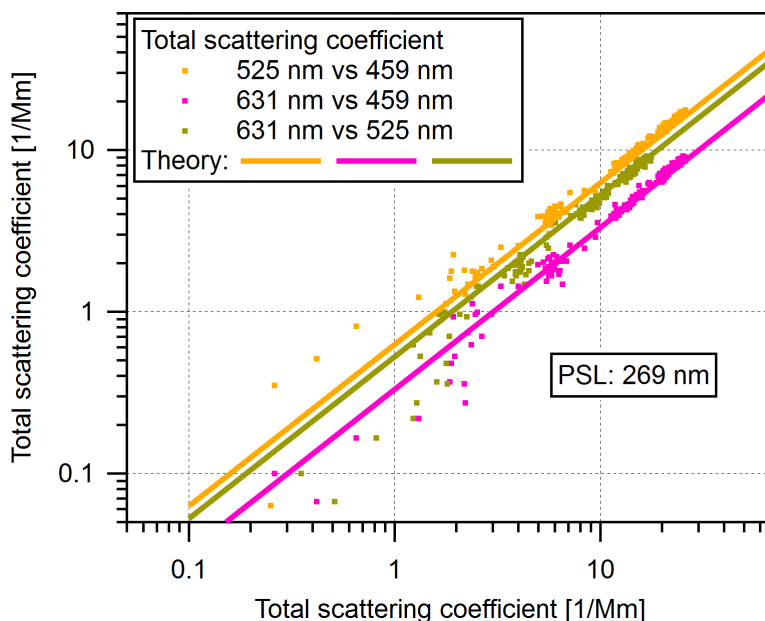
Fig. 2.3.6: Comparison of the experimental and theoretical response of the Airphoton IN101 nephelometer to PSL particles for the various wavelengths. The measured ratios between the different wavelengths have small deviation to the theoretical ones even at very low total scattering coefficients (< 5 Mm^{-1}), ensuring a reliable scattering Ångström exponent measurement.

2.4 Selected examples

2.4.1 Mechanisms of new particle formation

One scientific highlight from 2016 with contribution of the GAW monitoring data from JFJ is the high-profile article by Bianchi et al. (2016), providing new observational evidence about the mechanisms leading to new particle formation in the free troposphere. New particle formation (NPF) is the source of over half of the atmosphere's cloud condensation nuclei, thus influencing cloud properties and Earth's energy balance. Unlike in the planetary boundary layer, few observations of NPF in the free troposphere exist. The article by Bianchi et al. (2016) shows that at high altitudes, NPF occurs mainly through condensation of highly oxygenated molecules (HOMs), in addition to taking place through sulfuric acid–ammonia nucleation. Neutral nucleation is more than 10 times faster than ion-induced nucleation, and growth rates are size-dependent. NPF is restricted to a time window of 1 to 2 days after contact of the air masses with the planetary boundary layer; this is related to the time needed for oxidation of organic compounds to form HOMs. These findings require improved NPF parameterization in atmospheric models.

Three typical situations were identified, represented by consecutive example days (days 1 to 3) (Fig. 2.4.1.1); in addition, we show a special case (day 4) where the sulfuric acid concentration was unusually high (~6 × 10^6 cm^{-3}). Day 1 (25 February 2014) is an example of one of the many non-event days during sunny conditions. During the afternoon, there is a slight enhancement in the concentration of 5- to 10-nm particles, but the simultaneous increase in larger particles (up to 90 nm) suggests that this enhancement is related to vertical transport of particles formed elsewhere. Day 2 (26 February 2014) is typical of days when the JFJ is within clouds, when NPF is suppressed by reduced global radiation and the high condensation sink of the cloud droplets. Days 3 and 4 (27 February and 2 March 2014) are two examples of NPF days,

classified as 1A events, where the number concentration of particles larger than 3.2 nm increases strongly from a few hundred to 40,000 cm^{-3}.

On most sunny days, the sulfuric acid concentration followed a consistent diurnal cycle, with concentrations <10^4 cm^{-3} during the night and ≤5 × 10^5 cm^{-3} during the day (except day 4, which had much higher concentrations). However, no link was found between sulfuric acid and NPF, suggesting that sulfuric acid at these concentrations does not explain NPF at the JFJ (Fig. 2.4.1D). Highly oxygenated molecules (HOMs), which we detected with a chemical ionization–atmospheric pressure interface–time of flight mass spectrometer (CI-APi-TOF), were formed on some sunny days (e.g., day 3) but not on others (e.g., day 1) (Fig. 2.4.1D). This variability is probably dependent on the presence of organic precursors in the free troposphere. Figure . 2.4.1E shows the time evolution of several negative ions measured with an APi-TOF: HSO$_4^-$, NO$_3^-$, the family of clusters containing NH$_3$ and H$_2$SO$_4$, and ions with mass/charge ratios m/z > 400 Thomsons (Th; 1 Th = 1 Da e^{-1}, where e is the elementary charge), which are likely to be mainly organic compounds. Nucleation nearly exclusively occurred on days when the concentration of organic compounds was high. The nucleation event on day 4 had a somewhat different ion cluster composition; the organic ions were present, but HSO$_4^-$ and the H$_2$SO$_4$-NH$_3$ cluster family were of equal magnitude, probably because the H$_2$SO$_4$ concentration was very high (Fig. 2.4.1D). However, throughout the year of APi-TOF measurements, we never observed pure H$_2$SO$_4$ clusters with more than four molecules, confirming the findings of previous studies, which showed that binary H$_2$SO$_4$-H$_2$O nucleation does not explain atmospheric NPF.
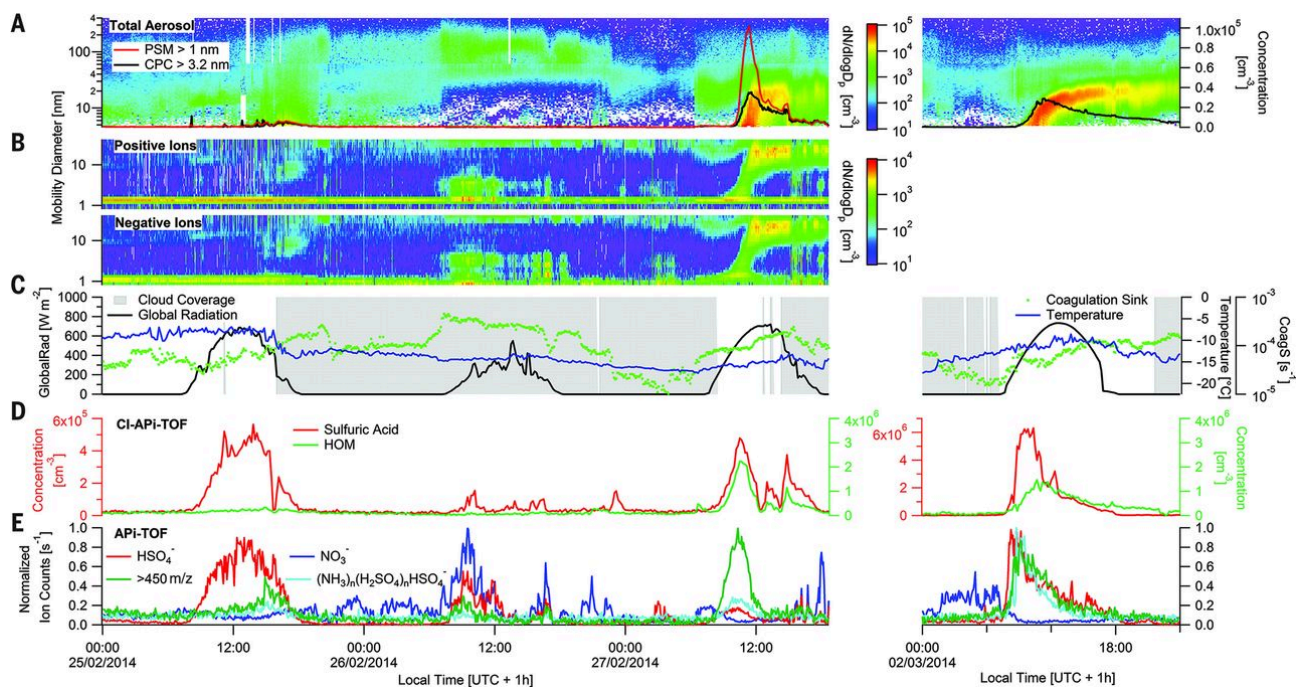
Fig. 2.4.1 Four representative situations observed at the JFJ. Shown are data from a sunny day with no nucleation (25 February, day 1), a cloudy day (26 February, day 2), a nucleation day with HOMs (27 February, day 3); and a nucleation day with H$_2$SO$_4$, NH$_3$, and HOMs (2 March, day 4) (h, hours). (A) Particle size distribution (dN/dlogDp), measured with a nano-SMPS (scanning mobility particle sizer), and particle number concentration above 1 and 3.2 nm, measured with a particle size magnifier (PSM) and a condensation particle counter (CPC), respectively. (B) Size distributions of the positive and negative ions measured by the NAIS. (C) Global radiation, temperature, coagulation sink, and cloud coverage. (D) Concentrations of sulfuric acid (red) and HOMs (green) measured with the CI-APi-TOF. A different axis is used for sulfuric acid in the right panel. (E) Measurements of specific ions with the APi-TOF (HSO$_4^-$ in red, NO$_3^-$ in blue, and the sum of ions with m/z >400 Th in green). The clusters containing sulfuric acid and ammonia are shown by the light blue line. Figure from Bianchi et al. (2016).

2.4.2 Climatology of the particle number size distribution at the Jungfraujoch

Figure 2.4.2.1 shows the mean seasonal pattern of the Aitken and accumulation mode properties (multimodal lognormal fits). The Aitken mode and accumulation mode diameters shown in Panel (a) only exhibit a very weak seasonality. For the 6-year measurement period from 2008–2014, the modal diameters of Aitken and accumulation mode were found to be 45 ± 11 nm (mean ± 1 SD) and 135 ± 26 nm, respectively (Herrmann et al., 2015). This is in good agreement with those observed by Weingartner et al. (1999) during the measurements in 1997/98. Similar to the total number concentration in Fig. 2.4.2.1 (e), the seasonal pattern of the integrated SMPS number concentration (Fig. 2.4.2.1 (b)) is due to the seasonality of the PBL influence (except for somewhat lower values due to higher cut-off diameter of the SMPS compared to the total number concentration measured by the CPC). Furthermore, Herrmann et al. (2015) also pointed out a clear *Hoppel* minimum around 80–90 nm in the number size distributions (Hoppel et al., 1986), indicating that the aerosol arriving at the JFJ typically experienced in-cloud processing during their travel, where particles above this diameter were activated and gained aerosol mass through aqueous phase processes.
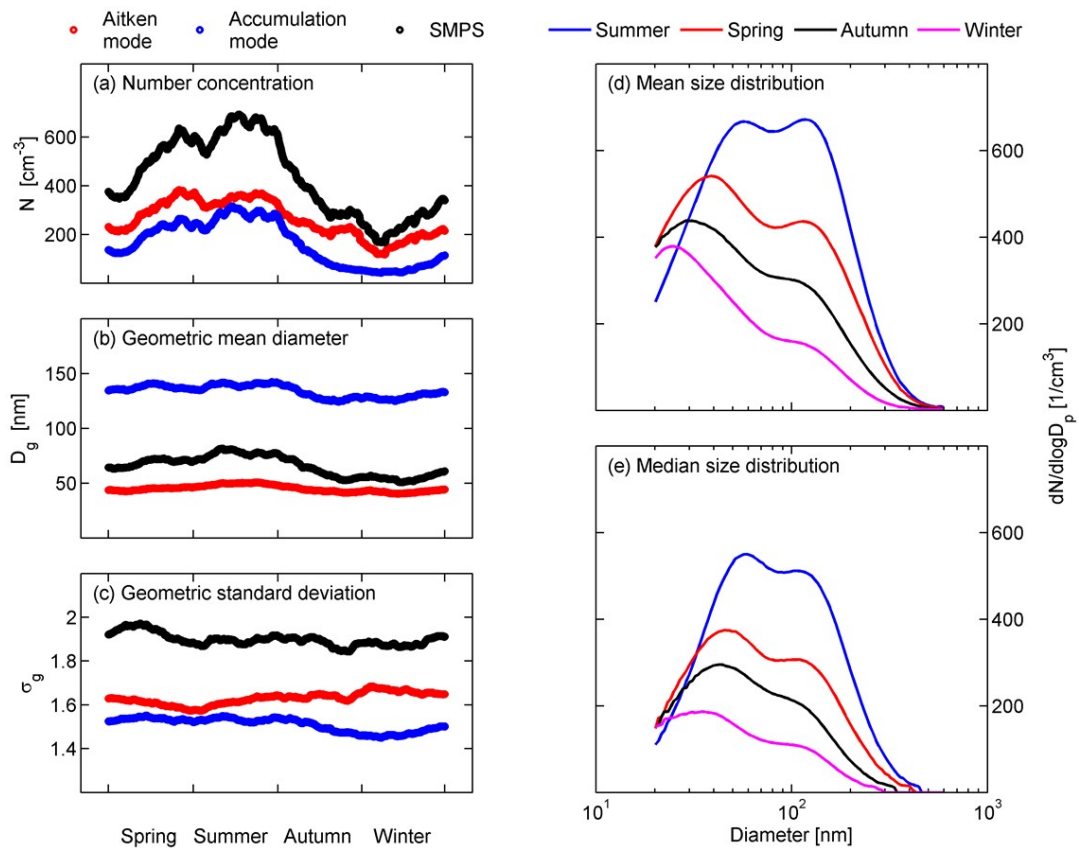
Fig. 2.4.2.1. Climatology and seasonal pattern of the aerosol number size distribution at the Jungfraujoch, adapted from Herrmann et al. (2015). The black lines in a), b) and c) show the integrated number concentration, the geometric mean diameter and the geometric standard deviation of the particle number size distribution, respectively (SMPS measurement between 20–600 nm). The red and blue lines in a), b), c) are the corresponding modal parameters of the Aitken and accumulation mode (obtained by multimodal lognormal fitting of 1h-average data followed by a 24 h moving median and averaging of seasonal cycles over 6 years).

2.4.3 Cloud condensation nuclei measurements

Our collected CCNC data are part of an ongoing effort to characterize CCN variability world-wide. While the initial step in the form of a synthesis of measurements within the FP6 project EUCAARI (Figure 2.4.3.1) has been completed, a new study goes one step ahead and provides a set of co-located particle number size distribution, CCN and aerosol composition data from long-term observations all over the globe (Schmale et al. 2017). This harmonized data set will serve as a benchmark for global model simulations.
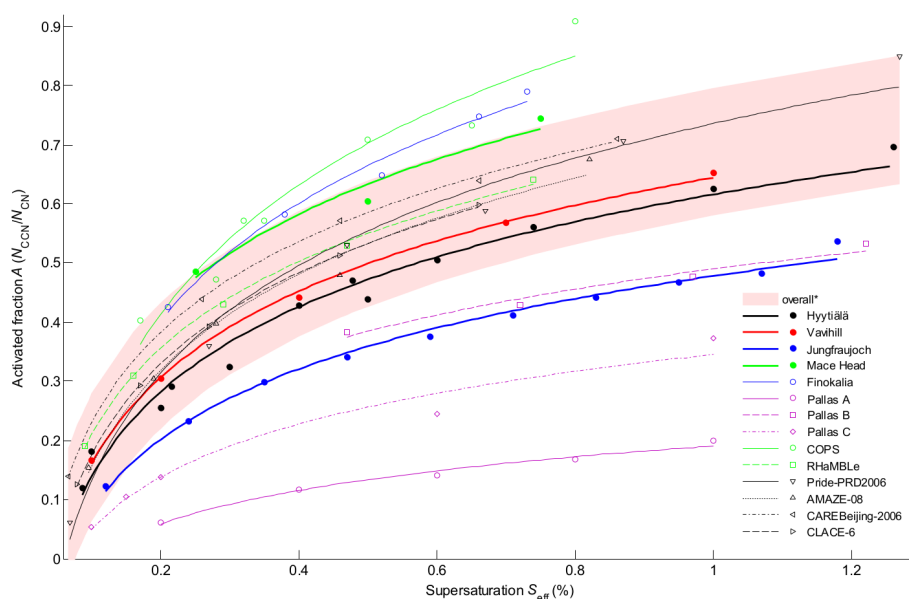
Fig. 2.4.3.1.: Average activated fraction A as a function of supersaturation S_{eff} for all available data sets. Lines represent linear fits in the form A = $a \times \ln(S_{eff})+b$. The shading of the overall fit represents the prediction bounds of the fit with a confidence level of 95 %.(from Paramonov et al., 2015).

2.4.4 Aerosol source apportionment based on online chemical analysis

Auxiliary financial resources made it possible to test a new aerosol mass spectrometer (ToF-ACSM) that was specifically developed for aerosol composition monitoring purposes in clean environments and with high time resolution. These tests revealed that the ToF-ACSM is indeed suitable for this purpose. Furthermore, these data were successfully used to determine the contributions of various sources to the organic aerosol by means of statistical analyses such as positive matrix factorization. This is an important new achievement, which was so far only possible with much more complex research instruments.

Fröhlich et al. (2015) present chemically resolved (organic, nitrate, sulfate, ammonium) data of non-refractory submicron (NR-PM1) aerosol from the first long-term deployment (27 July 2012 to 02 October 2013) of a time-of-flight aerosol chemical speciation monitor (ToF-ACSM) at the Jungfraujoch. Backward transport simulations show that the highest (especially sulfate) concentrations of NR-PM1 were measured in air

masses advected to the station from regions south of the JFJ, while lowest concentrations were seen from western regions. The organic aerosol (OA) was dominated in all seasons by oxygenated OA (OOA, 71–88 %), with lesser contributions from local tourism-related activities (7–12 %) and hydrocarbon-like OA related to regional vertical transport (3–9 %). Wood burning-related OA associated with regional transport was detected during the whole winter 2012/2013 and during rare events in summer 2013, in the latter case attributed to small-scale transport for the surrounding valleys. Additionally, the data were divided into periods with free tropospheric (FT) conditions and periods with planetary boundary layer (PBL) influence, enabling the assessment of the composition for each. Most nitrate and part of the OA are injected from the regional PBL, while sulfate is mainly produced in the FT. The south/north gradient of sulfate is also pronounced in FT air masses (sulfate mass fraction from the south: 45 %; from the north: 29 %).
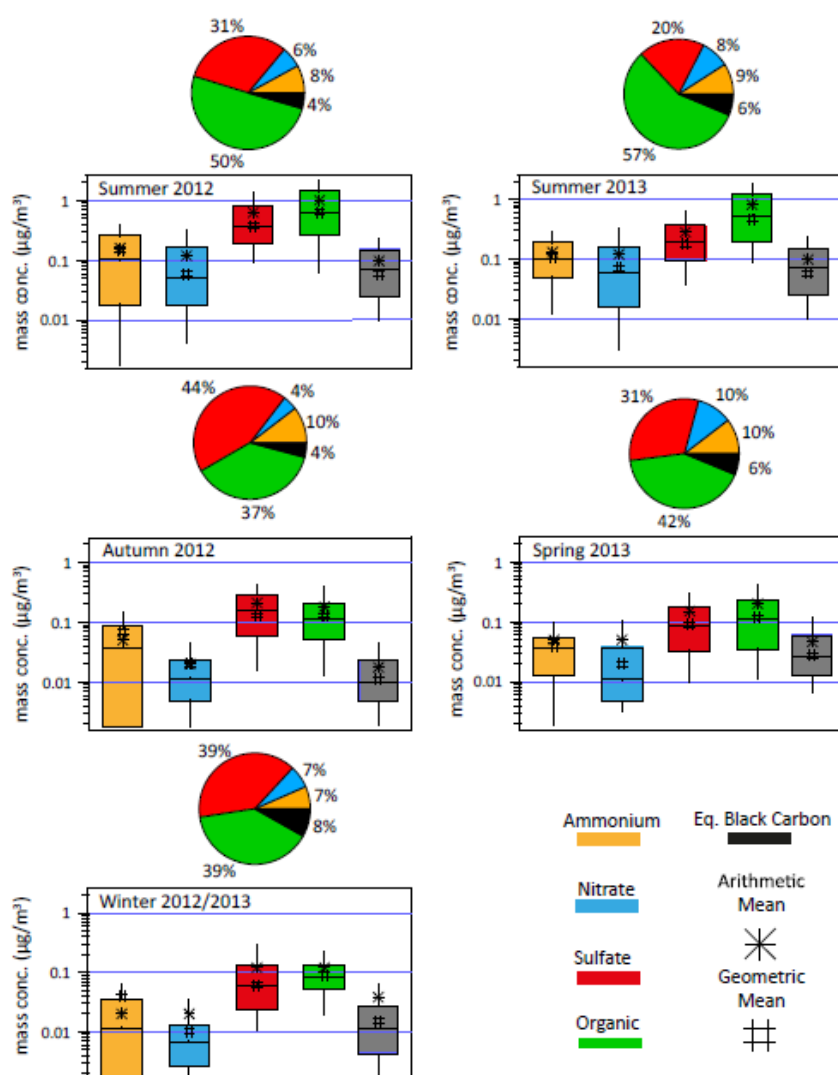
Fig. 2.4.4.1.: Pie charts of the relative average concentration and boxplots (in µg m⁻³; line: median; box: interquartile range; whiskers: 10–90th percentile range) separated by seasons (summer 2012, autumn 2012, winter 2012/2013, spring 2013 and summer 2013) for species measured with the ACSM (organic: green; sulfate: red; nitrate: blue; and ammonium: orange) and eBC derived from optical absorption measurements. The arithmetic mean of each species is indicated by a star and the geometric mean by a hash in the respective boxplot. Mean and median concentration values for each species and season can be found in Table 1. Relative concentrations are given in percent in the pie charts.

2.4.5 The topography contribution to the influence of the planetary boundary layer at high altitude stations

High altitude stations are often emphasized as free tropospheric measuring sites but they remain influenced by atmospheric boundary layer (ABL) air masses due to convective transport processes. A topography analysis was then performed allowing calculation of a newly defined index called ABL-TopoIndex (Collaud Coen et al., 2017). The ABL-TopoIndex is constructed in order to correlate with the ABL influence at the high altitude stations and long-term aerosol time series are used to assess its validity. Other important parameters influencing the aerosol load such as the wind, the soil state and the synoptic weather conditions were not taken into account.

43 high altitude stations representative of 5 continents were analysed . The ABL-TopoIndex relies on the criteria that the ABL influence will be low if 1) the station is one of the highest points in the mountainous massif, 2) there is a large altitude difference between the station and the valleys, plateaus or the average domain elevation, 3) the slopes around the station are steep, and 4) the «drainage basin» for air convection is small. These principles are implemented by the calculation of 5 parameters involving the hypsometric curve, the steepness of the slopes around the station and the drainage basin for convection. The geometrical mean of these five parameters is the ABL-TopoIndex and allows ranking of the stations as a function of the ABL influence due to convection.

The first observation is that all stations on volcanic islands (in this study) have very low ABL-TopoIndex (i.e., low BL influence), whereas the stations in the Himalaya and the Tibetan plateau have high ABL-TopoIndex. The highest research stations in the alps have low ABL-TopoIndex, the JFJ being the alpine station with least ABL influence.

Statistically significant correlations between the ABL-TopoIndex and the aerosol parameters measured at 28 high altitude sites allow validation of the methodological approach. The greatest correlations are found with the minima of the aerosol parameters that represent the most likely FT air masses. The maxima of aerosol parameters are more representative of the intensity of aerosol sources and of advection of air masses with high aerosol concentrations. There are also strong anti-correlations between the slope local steepness and the particle number concentration, suggesting that new particle formation could be largely influenced by this topographical parameter. The amplitude of the diurnal cycle of the absorption coefficient is also correlated with the ABL-TopoIndex and is, thus, likely to be representative of ABL influence. The strength of the diurnal cycles of the scattering coefficient and the number concentration are, however, mostly explained by the latitude of the station, leading to the conclusion that the insolation drives the aerosol diurnal cycle.
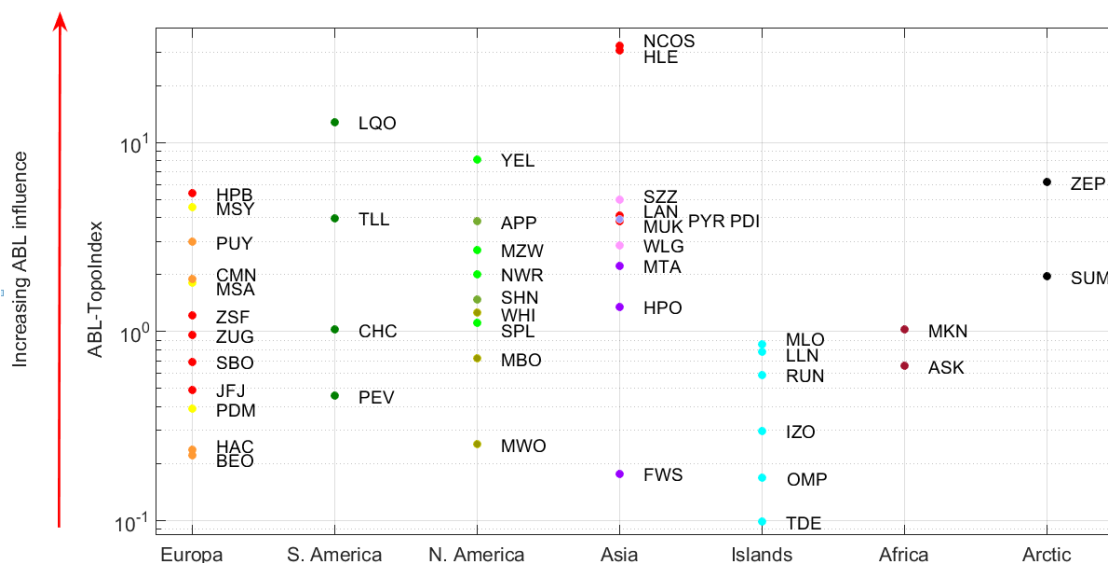
Fig. 2.4.5.1: ABL-TopoIndex for all stations as a function of continents and mountainous ranges

3 Papers related to the GAW-CH program published 2014 - 2017

3.1 Published peer reviewed papers

2017:

Frege, C., Bianchi, F., Molteni, U., Tröstl, J., Junninen, H., Henne, S., Sipilä, M., Herrmann, E., Rossi, M. J., Kulmala, M., Hoyle, C. R., Baltensperger, U., and Dommen, J.: Chemical characterization of atmospheric ions at the high altitude research station Jungfraujoch (Switzerland), Atmos. Chem. Phys., 17, 2613-2629, https://doi.org/10.5194/acp-17-2613-2017, 2017.

Lacher, L., Lohmann, U., Boose, Y., Zipori, A., Herrmann, E., Bukowiecki, N., Steinbacher, M., and Kanji, Z. A.: The Horizontal Ice Nucleation Chamber (HINC): INP measurements at conditions relevant for mixed-phase clouds at the High Altitude Research Station Jungfraujoch, Atmos. Chem. Phys., 17, 15199-15224, https://doi.org/10.5194/acp-17-15199-2017, 2017.

Poltera, Y., Martucci, G., Collaud Coen, M., Hervo, M., Emmenegger, L., Henne, S., Brunner, D., and Haefele, A.: PathfinderTURB: an automatic boundary layer algorithm. Development, validation and application to study the impact on in situ measurements at the Jungfraujoch, Atmos. Chem. Phys., 17, 10051-10070, https://doi.org/10.5194/acp-17-10051-2017, 2017.

Schmale, J., Henning, S., Henzing, B., Keskinen, H., Sellegri, K., Ovadnevaite, J., Bougiatioti, A., Kalivitis, N., Stavroulas, L., Jefferson, A., Park, M., Schlag, P., Kristensson, A., Iwamotol, Y., Pringle, K., Reddington, C., Aalto, P., Aijala, M., Baltensperger, U., Bialek, J., Birmili, W., Bukowiecki, N., Ehn, M., Fjaeraa, A., M., Fiebig, M., Frank, G., Frohlich, R., Frumau, A., Furuyals, M., Hammer, E., Heikkinen, L., Herrmann, E., Holzinger, R., Hyonols, H., Kanakidoug, M., Kiendler-Scharr, A., Kinouchi, K., Kos, G., Kulmala, M., Mihalopoulos, N., Motos, G., Nenes, A., O'Dowd, C., Paramonov, M., Petaja, T., Picard, D., Poulain, L., Prevot, A. S. H., Slowik, J., Sonntag, A., Swietlicki, E., Svenningsson, B., Tsurumaru, H., Wiedensohler, A., Wittbom, C., Ogren, J. A., Matsuki, A., Yum, S. S., Myhre, C. L., Carslaw, K., Stratmann, F., and Gysel, M., Data Descriptor: Collocated observations of cloud condensation nuclei, particle size distributions, and

chemical composition, Scientific Data., 4, Article number: 170003, https://doi.org/ doi:10.1038/sdata.2017.3, 2017.

Schmidt, S., Schneider, J., Klimach, T., Mertes, S., Schenk, L. P., Kupiszewski, P., Curtius, J., and Borrmann, S.: Online single particle analysis of ice particle residuals from mountain-top mixed-phase clouds using laboratory derived particle type assignment, Atmos. Chem. Phys., 17, 575-594, https://doi.org/10.5194/acp-17-575-2017, 2017.

2016:

Bianchi, F., Tröstl, J., Junninen, H., Frege, C., Henne, S., Hoyle, C. R., Molteni, U., Herrmann, E., Adamov, A., Bukowiecki, N., Chen, X., Duplissy, J., Gysel, M., Hutterli, M., Kangasluoma, J., Kontkanen, J., Kürten, A., Manninen, H. E., Münch, S., Peräkylä, O., Petäjä, T., Rondo, L., Williamson, C., Weingartner, E., Curtius, J., Worsnop, D. R., Kulmala, M., Dommen, J., and Baltensperger, U.: New particle formation in the free troposphere: A question of chemistry and timing. Science, **352**, 1109-1112, doi:10.1126/science.aad5456, 2016.

Boose, Y., Kanji, Z. A., Kohn, M., Sierau, B., Zipori, A., Crawford, I., Lloyd, G., Bukowiecki, N., Herrmann, E., Kupiszewski, P., Steinbacher, M., and Lohmann, U.: Ice nucleating particle measurements at 241 K during winter months at 3580 m MSL in the Swiss Alps. J. Atmos. Sci., **73**, 2203-2228, doi:10.1175/JAS-D-15-0236.1, 2016.

Bukowiecki, N., Weingartner, E., Gysel, M., Collaud Coen, M., Zieger, P., Herrmann, E., Steinbacher, M., Gäggeler, H. W., and Baltensperger, U.: A review of more than 20 years of aerosol observation at the high altitude research station Jungfraujoch, Switzerland (3580 m asl). Aerosol Air Qual. Res., **16**, 764–788, doi:10.4209/aaqr.2015.05.0305, 2016.

Crawford, I., Lloyd, G., Herrmann, E., Hoyle, C. R., Bower, K. N., Connolly, P. J., Flynn, M. J., Kaye, P. H., Choularton, T. W., and Gallagher, M. W.: Observations of fluorescent aerosol–cloud interactions in the free troposphere at the High-Altitude Research Station Jungfraujoch. Atmos. Chem. Phys., **16**, 2273-2284, doi:10.5194/acp-16-2273-2016, 2016.

Hoyle, C. R., Webster, C. S., Rieder, H. E., Nenes, A., Hammer, E., Herrmann, E., Gysel, M., Bukowiecki, N., Weingartner, E., Steinbacher, M., and Baltensperger, U.: Chemical and physical influences on aerosol activation in liquid clouds: a study based on observations from the Jungfraujoch, Switzerland. Atmos. Chem. Phys., **16**, 4043-4061, doi:10.5194/acp-16-4043-2016, 2016.

Kupiszewski, P., Zanatta, M., Mertes, S., Vochezer, P., Lloyd, G., Schneider, J., Schenk, L., Schnaiter, M., Baltensperger, U., Weingartner, E., and Gysel, M.:. Ice residual properties in mixed-phase clouds at the high-alpine Jungfraujoch site, J. Geophys. Res. Atmos., 121, 12,343–12,362, doi:10.1002/2016JD024894, 2016.

Rosati, B., Herrmann, E., Bucci, S., Fierli, F., Cairo, F., Gysel, M., Tillmann, R., Größ, J., Gobbi, G. P., Di Liberto, L., Di Donfrancesco, G., Wiedensohler, A., Weingartner, E., Virtanen, A., Mentel, T. F., and Baltensperger, U.: Studying the vertical aerosol extinction coefficient by comparing in situ airborne data and elastic backscatter lidar. Atmos. Chem. Phys., 16, 4539-4554, doi:10.5194/acp-16-4539-2016, 2016.

Stopelli, E., Conen, F., Morris, C. E., Herrmann, E., Henne, S., Steinbacher, M., and Alewell, C.: Predicting abundance and variability of ice nucleating particles in precipitation at the high-altitude observatory Jungfraujoch. Atmos. Chem. Phys., **16**, 8341-8351, doi:10.5194/acp-16-8341-2016, 2016.

Tröstl, J., Frege, C., Bianchi, F., Molteni, U., Bukowiecki, N., Hoyle, C.R., Steinbacher, M., Weingartner, E., Dommen, J., Gysel, Martin and Baltensperger, U.: Contribution of new particle formation to the total aerosol concentration at the high-altitude site Jungfraujoch (3580 m asl, Switzerland), J. Geophys. Res. Atmos., 121, 11,692–11,711, doi:10.1002/2015JD024637, 2016.

Vochezer, P., Järvinen, E., Wagner, R., Kupiszewski, P., Leisner, T., and Schnaiter, M.: In situ characterization of mixed phase clouds using the Small Ice Detector and the Particle Phase Discriminator. Atmos. Meas. Tech., **9**, 159-177, doi:10.5194/amt-9-159-2016, 2016.

Conen, F., Rodríguez, S., Hüglin, C., Henne, S., Herrmann, E., Bukowiecki, N., and Alewell, C.: Atmospheric ice nuclei at the high-altitude observatory Jungfraujoch, Switzerland, Tellus B, 67, 25014, doi:10.3402/tellusb.v67.25014, 2015.

Crawford, I., Lloyd, G., Herrmann, E., Hoyle, C. R., Bower, K. N., Connolly, P. J., Flynn, M. J., Kaye, P. H., Choularton, T. W., and Gallagher, M. W.: Observations of fluorescent aerosol–cloud interactions in the free troposphere at the High-Altitude Research Station Jungfraujoch, Atmos. Chem. Phys., 16, 2273-2284, doi:10.5194/acp-16-2273-2016, 2016.

2015:

Fröhlich, R., Cubison, M. J., Slowik, J. G., Bukowiecki, N., Canonaco, F., Croteau, P. L., Gysel, M., Henne, S., Herrmann, E., Jayne, J. T., Steinbacher, M., Worsnop, D. R., Baltensperger, U., and Prévôt, A. S. H.: Fourteen months of on-line measurements of the non-refractory submicron aerosol at the Jungfraujoch (3580 m a.s.l.) – chemical composition, origins and organic aerosol sources, Atmos. Chem. Phys., 15, 11373-11398, doi:10.5194/acp-15-11373-2015, 2015.

Grazioli, J., Lloyd, G., Panziera, L., Hoyle, C. R., Connolly, P. J., Henneberger, J., and Berne, A.: Polarimetric radar and in situ observations of riming and snowfall microphysics during CLACE 2014, Atmos. Chem. Phys., 15, 13787-13802, doi:10.5194/acp-15-13787-2015, 2015.

Hammer, E., Bukowiecki, N., Luo, B. P., Lohmann, U., Marcolli, C., Weingartner, E., Baltensperger, U., and Hoyle, C. R.: Sensitivity estimations for cloud droplet formation in the vicinity of the high-alpine research station Jungfraujoch (3580 m a.s.l.), Atmos. Chem. Phys., 15, 10309-10323, doi:10.5194/acp-15-10309-2015, 2015.

Herrmann, E., Weingartner, E., Bukowiecki, N., Hammer, E., Jurányi, Z., Collaud Coen, M., Vuilleumier, L., Steinbacher, M., Henne, S., Conen, F., Baltensperger, U., and Gysel, M.: Analysis of long-term aerosol size distribution data from Jungfraujoch with emphasis on free tropospheric conditions, cloud influence, and air mass transport, J. Geophys. Res.-Atmos., 120, 9459-9480, doi:10.1002/2015JD023660, 2015.

Kupiszewski, P., Weingartner, E., Vochezer, P., Schnaiter, M., Bigi, A., Gysel, M., Rosati, B., Toprak, E., Mertes, S., and Baltensperger, U.: The Ice Selective Inlet: a novel technique for exclusive extraction of pristine ice crystals in mixed-phase clouds, Atmos. Meas. Tech., 8, 3087–3106, doi:10.5194/amt-8-3087-2015, 2015.

Paramonov, M., Kerminen, V.-M., Gysel, M., Aalto, P. P., Andreae, M. O., Asmi, E., Baltensperger, U., Bougiatioti, A., Brus, D., Frank, G. P., Good, N., Gunthe, S. S., Hao, L., Irwin, M., Jaatinen, A., Jurányi, Z., King, S. M., Kortelainen, A., Kristensson, A., Lihavainen, H., Kulmala, M., Lohmann, U., Martin, S. T., McFiggans, G., Mihalopoulos, N., Nenes, A., O'Dowd, C. D., Ovadnevaite, J., Petäjä, T., Pöschl, U., Roberts, G. C., Rose, D., Svenningsson, B., Swietlicki, E., Weingartner, E., Whitehead, J., Wiedensohler, A., Wittbom,

C., and Sierau, B.: A synthesis of cloud condensation nuclei counter (CCNC) measurements within the EUCAARI network, Atmos. Chem. Phys., 15, 12211-12229, doi:10.5194/acp-15-12211-2015, 2015.

Stopelli, E., Conen, F., Morris, C. E., Herrmann, E., Bukowiecki, N., and Alewell, C.: Ice nucleation active particles are efficiently removed by precipitating clouds, Sci. Rep. 5, 16433, doi:10.1038/srep16433, 2015.

Vochezer, P., Järvinen, E., Wagner, R., Kupiszewski, P., Leisner, T., and Schnaiter, M.: In situ characterization of mixed phase clouds using the Small Ice Detector and the Particle Phase Discriminator, Atmos. Meas. Tech. , 9, 159-177, doi:10.5194/amt-9-159-2016 , 2016.

Worringen, A., Kandler, K., Benker, N., Dirsch, T., Mertes, S., Schenk, L., Kästner, U., Frank, F., Nillius, B., Bundke, U., Rose, D., Curtius, J., Kupiszewski, P., Weingartner, E., Vochezer, P., Schneider, J., Schmidt, S., Weinbruch, S., and Ebert, M.: Single-particle characterization of ice-nucleating particles and ice particle residuals sampled by three different techniques, Atmos. Chem. Phys., 15, 4161–4178, doi:10.5194/acp-15-4161-2015, 2015.

2014:

Beddows, D. C. S., Dall'Osto, M., Harrison, R. M., Kulmala, M., Asmi, A., Wiedensohler, A., Laj, P., Fjaeraa, A. M., Sellegri, K., Birmili, W., Bukowiecki, N., Weingartner, E., Baltensperger, U., Zdimal, V., Zikova, N., Putaud, J.-P., Marinoni, A., Tunved, P., Hansson, H.-C., Fiebig, M., Kivekäs, N., Swietlicki, E., Lihavainen, H., Asmi, E., Ulevicius, V., Aalto, P. P., Mihalopoulos, N., Kalivitis, N., Kalapov, I., Kiss, G., de Leeuw, G., Henzing, B., O'Dowd, C., Jennings, S. G., Flentje, H., Meinhardt, F., Ries, L., Denier van der Gon, H. A. C., and Visschedijk, A. J. H.: Variations in tropospheric submicron particle size distributions across the European continent 2008–2009. Atmos. Chem. Phys., 14, 4327-4348, doi:10.5194/acp-14-4327-2014, 2014.

Conen, F., Rodruguez, S., Hüglin, C., Henne, S., Herrmann, E., Bukowiecki, N., and Alewell, C.: Atmospheric ice nuclei at the high-altitude observatory Jungfraujoch, Switzerland, Tellus B 2015, 67, 25014, doi:10.3402/tellusb.v67.25014

Hammer, E., Bukowiecki, N., Gysel, M., Jurányi, Z., Hoyle, C. R., Vogt, R., Baltensperger, U., and Weingartner, E.: Investigation of the effective peak supersaturation for liquid-phase clouds at the high-alpine site Jungfraujoch, Switzerland (3580 m a.s.l.), Atmos. Chem. Phys., 14, 1123-1139, doi:10.5194/acp-14-1123-2014, 2014.

Hammer, E., Bukowiecki, N., Luo, B. P., Lohmann, U., Marcolli, C., Weingartner, E., Baltensperger, U., and Hoyle, C. R.: Sensitivity estimations for cloud droplet formation in the vicinity of the high alpine research station Jungfraujoch (3580 m a.s.l.), Atmos. Chem. Phys. Discuss., 14, 25967-26002, doi:10.5194/acpd-14-25967-2014, 2014.

Ketterer, C., Zieger, P., Bukowiecki, N., Collaud Coen, M., Maier, O., Ruffieux, D., and Weingartner, E.: Investigation of the planetary boundary layer in the Swiss alps using remote sensing and in situ measurements. Bound.-Lay. Meterol., 151, 317-334, doi:10.1007/s10546-013-9897-8, 2014.

Kupiszewski, P., Weingartner, E., Vochezer, P., Bigi, A., Rosati, B., Gysel, M., Schnaiter, M., and Baltensperger, U.: The Ice Selective Inlet: a novel technique for exclusive extraction of pristine ice crystals in mixed-phase clouds, Atmos. Meas. Tech. Discuss., 7, 12481-12515, doi:10.5194/amtd-7-12481-2014, 2014.

Mann, G. W., Carslaw, K. S., Reddington, C. L., Pringle, K. J., Schulz, M., Asmi, A., Spracklen, D. V., Ridley, D. A., Woodhouse, M. T., Lee, L. A., Zhang, K., Ghan, S. J., Easter, R. C., Liu, X., Stier, P., Lee, Y. H., Adams, P. J., Tost, H., Lelieveld, J., Bauer, S. E., Tsigaridis, K., van Noije, T. P. C., Strunk, A., Vignati, E.,

Bellouin, N., Dalvi, M., Johnson, C. E., Bergman, T., Kokkola, H., von Salzen, K., Yu, F., Luo, G., Petzold, A., Heintzenberg, J., Clarke, A., Ogren, J. A., Gras, J., Baltensperger, U., Kaminski, U., Jennings, S. G., O'Dowd, C. D., Harrison, R. M., Beddows, D. C. S., Kulmala, M., Viisanen, Y., Ulevicius, V., Mihalopoulos, N., Zdimal, V., Fiebig, M., Hansson, H.-C., Swietlicki, E., and Henzing, J. S.: Intercomparison and evaluation of global aerosol microphysical properties among AeroCom models of a range of complexity, Atmos. Chem. Phys., 14, 4679-4713, doi:10.5194/acp-14-4679-2014, 2014.